

Rigorous Numerical Study of Low-Period Windows for the Quadratic Map

Zbigniew Galias

Department of Electrical Engineering,
AGH University of Science and Technology,
Mickiewicza 30, 30–059 Kraków, Poland
galias@agh.edu.pl

An efficient method to find all low-period windows for the quadratic map is proposed. The method is used to obtain very accurate rigorous bounds of positions of all periodic windows with periods $p \leq 32$. The contribution of period-doubling windows on the total width of periodic windows is discussed. Properties of periodic windows are studied numerically.

Keywords: Quadratic map; logistic map; periodic window; interval Newton operator; interval arithmetic.

1. Introduction

The *quadratic map* $f_a(x) = ax(1 - x)$ (often also called the *logistic map*) [May, 1976] is a classical example of a nonlinear dynamical system that can exhibit complex behaviours. In the parameter space $\mathcal{S} = [0, 4]$ of the quadratic map one can define sets $\mathcal{S}_{\text{periodic}}$ and $\mathcal{S}_{\text{chaotic}}$ of parameter values for which there exist a periodic attractor or a chaotic attractor, respectively. It is known that these two sets are disjoint and their measures are positive [Day *et al.*, 2008]. The measure of the set $\mathcal{S} \setminus (\mathcal{S}_{\text{periodic}} \cup \mathcal{S}_{\text{chaotic}})$ is zero [Lyubich, 2002], i.e. for almost every parameter either a chaotic or periodic attractor exist. Parameter values not belonging to either of these two sets correspond to saddle-node and period-doubling bifurcation points and to period-doubling cascade accumulation points. These points constitute a countable set and therefore its measure is zero.

The goal of this work is numerical study the set $\mathcal{S}_{\text{periodic}}$. This set can be split into an infinite number of pairwise disjoint sets $\mathcal{S}_{\text{periodic},p}$, $p = 1, 2, \dots$, where $\mathcal{S}_{\text{periodic},p}$ contains parameter values for which a stable period- p orbit exists. For the quadratic map it is known that each of these sets is a union of open intervals, which are called periodic windows. Hence, in order to compute a measure of the set $\mathcal{S}_{\text{periodic},p}$ for a given p one has to find all period- p windows. Periodic windows can be found analytically only for very low periods. The bisection method to find periodic windows for the quadratic map has been used in [Tucker & Wilczak, 2009]. In this method, the interval of parameter values is split into smaller parts, the Newton method is used to find superstable orbits in each part and then the regions found are extended to cover as much of a periodic window as possible. In [Tucker & Wilczak, 2009], the results on widths of periodic windows found were used to obtain a lower bound on the measure of the set $\mathcal{S}_{\text{periodic}}$. By construction, the method described in [Tucker & Wilczak, 2009] finds only periodic windows with widths above a given threshold. Another limitation of this method is that it only finds a lower bound of windows' width. In [Galias & Garda, 2015], the continuation method was used to find positions of all periodic windows with periods $p \leq 20$. For each periodic window a rigorous lower bound of the window width was found using the forward shooting based interval Newton operator to confirm the existence of stable periodic orbits for parameter values close to window endpoints.

In this work, we continue research in this direction. We present a systematic method to find all low-period

windows with a very good accuracy. The method is capable of computing both lower and upper bounds of widths of each periodic window. It is shown that the method is faster than the one used in [Galias & Garda, 2015]. As a result we are able to find all periodic windows up to period 32. It is shown that the accuracy of the method is also improved. This method guarantees that all windows of a given period are found and therefore can be used to compute rigorously very accurate bounds for the measures of sets $\mathcal{S}_{\text{periodic},p}$ for small p .

The layout of the paper is as follows. In Sec. 2, several properties of periodic windows for the quadratic map are recalled. In Sec. 3, the search method is described in detail and in Sec. 4, results of applying this method to analyse low-period windows for the quadratic map are presented. Throughout the paper, we will use bold face to denote intervals, interval vectors and matrices and math italic to denote “real” quantities. The interval with endpoints $\underline{x} \leq \bar{x}$ is defined as $\mathbf{x} = [\underline{x}, \bar{x}]$. The diameter of the interval \mathbf{x} is defined as $\text{diam}(\mathbf{x}) = \bar{x} - \underline{x}$. To define intervals we will sometimes use a shorter notation. For example, $\mathbf{x} = 3.44_{55}^{67}$ will denote the interval $\mathbf{x} = [3.4455, 3.4467]$. An interval vector is a Cartesian product of intervals, for example $\mathbf{x} = (\mathbf{x}_1, \dots, \mathbf{x}_n)^\top = \mathbf{x}_1 \times \dots \times \mathbf{x}_n$.

2. Preliminaries

The quadratic map is a one-parameter map of the interval $I = [0, 1]$ defined by

$$f_a(x) = ax(1 - x), \quad (1)$$

where $a \in \mathcal{S} = [0, 4]$.

We say that x_0 is a *period- p point* of f_a if $f_a^p(x_0) = x_0$, and $f_a^k(x_0) \neq x_0$ for $1 \leq k < p$, where the notation $f_a^0(x_0) = x_0$ and $f_a^{k+1}(x_0) = f_a(f_a^k(x_0))$ for $k \geq 0$ is used. The corresponding trajectory $x_k = f_a^k(x)$, $k \geq 0$ is called a *periodic orbit*. We say that the periodic orbit $(x_0, x_1, \dots, x_{p-1})$ is *stable* (is a *sink*) if the derivative

$$\lambda_p(a, x_0) = (f_a^p(x_0))' = \prod_{k=0}^{p-1} f_a'(x_k) = \prod_{k=0}^{p-1} a(1 - 2x_k), \quad (2)$$

is smaller than one in absolute value.

Let us recall some well known results on periodic windows for the quadratic map which will be used in this work. For details the reader is referred to introductory books on deterministic chaos, for example [Peitgen *et al.*, 2004].

We say that an open interval $(a_{\text{left}}, a_{\text{right}}) \subset \mathcal{S}$ is a *period- p window* for the family $\{f_a : a \in \mathcal{S}\}$ if for all $a \in (a_{\text{left}}, a_{\text{right}})$ there exists a period- p sink of f_a , and $(a_{\text{left}}, a_{\text{right}})$ is a maximal interval with this property. Endpoints of periodic windows are bifurcation points of corresponding periodic orbits. Periodic windows for which at the left endpoint there is a saddle-node/period-doubling bifurcation will be referred to as *saddle-node* windows and *period-doubling* windows, respectively. For the quadratic map there is a period-doubling bifurcation at the right endpoint of each periodic window, and at this point another periodic window (of period-doubling type) starts. Thus, each saddle-node window generates an infinite sequence of periodic windows with common endpoints. Such a sequence is called a *period-doubling cascade*.

Let us consider a fixed value of the parameter a . With the point $x \in [0, 1]$ we associate the *symbol sequence* $s(x) = s = (s_0, s_1, \dots)$ in such a way that $s_k = 0$ if $x_k < 0.5$ and $s_k = 1$ if $x_k \geq 0.5$, where (x_0, x_1, x_2, \dots) is the trajectory of f_a with the initial point $x_0 = x$, i.e. $x_k = f_a^k(x)$. If x is a period- p point then s is also periodic. In such a case, we will write for short $s = (s_0, s_1, \dots, s_{p-1})$.

Positions of periodic orbits of f_a for $a = 4$ can be found using the topological conjugacy between $f_{4,0}$ and the *tent map* $T : [0, 1] \mapsto [0, 1]$ defined by $T(y) = 1 - |2y - 1|$. The homeomorphism conjugating $f_{4,0}$ and T is given by

$$x = h(y) = \sin^2(0.5\pi y). \quad (3)$$

For each periodic symbol sequence $s = (s_0, s_1, \dots, s_{p-1})$ of period p there exists exactly one point y_0 such that $T^p(y_0) = y_0$ and the symbol sequence of y_0 is s . Its position can be found using the formula

$$y_0 = \left(1 - 2^{-2p}\right)^{-1} \sum_{i=0}^{2p-1} t_i 2^{-i-1}, \quad t_k = \left(\sum_{i=0}^k s_i\right) \bmod 2. \quad (4)$$

The homeomorphism h converts trajectories of T into trajectories of $f_{4,0}$, i.e. $f_{4,0}^k(h(y)) = h(T^k(y))$ for $k \geq 0$ and $y \in [0, 1]$. Hence, $x_0 = h(y_0)$ is the position of the period- p point of $f_{4,0}$ corresponding to the symbol sequence s . For

example when $p = 3$ and $s = (001)$, we obtain $t = (001110)$, $y_0 = 2/9$, $x_0 = \sin^2(0.5\pi y_0) \approx 0.11697777844$, which is a period-3 point of $f_{4.0}$.

The number of fixed points of $f_{4.0}^p$ is 2^p . These fixed points correspond to periodic orbits of f_a with period p and its proper divisors. Therefore, the number $P(p)$ of period- p orbits of $f_{4.0}$ can be found using the following recursive formula

$$P(p) = p^{-1} \left(2^p - \sum_{k=1, p \bmod k=0}^{p-1} k \cdot P(k) \right). \quad (5)$$

Periodic points of $f_{4.0}$ are all unstable. For $y \neq 0.5$ we have $|T'(y)| = 2$. It follows that the derivative of a fixed point y_0 of T^p is $(T^p(y_0))' = T'(y_{p-1}) \cdots T'(y_1)T'(y_0) = \pm 2^p$. The sign depends on the parity of the number of points for which $s_k = 1$ (at these points $T'(y_k) = -2$). Since the derivative of a fixed point is invariant under the change of coordinates, it follows that for x_0 being a fixed point of $f_{4.0}^p$ we have $\lambda_p(4.0, x_0) = (f_{4.0}^p(x_0))' = (-1)^{t_{p-1}} 2^p$, where $s = s(x_0)$ is the symbol sequence of x_0 , and t_{p-1} is defined in (4). We will refer to period- p symbol sequences for which the number of nonzero symbols is odd as *odd-parity sequences*.

Let us consider a period- p orbit $(x_0, x_1, \dots, x_{p-1})$ of $f_{4.0}$, and let $s = s(x_0)$ be the corresponding symbol sequence. When a is decreased, the position $(x_k(a))_{k=0}^{p-1}$ of the periodic orbit changes until at some point a_{left} the derivative $\lambda_p(a, x_0(a))$ reaches 1. For odd-parity sequences $\lambda_p(4.0, x) < -1$ and in consequence there exist $a_{\text{right}} > a_{\text{left}}$ such that $\lambda_p(a_{\text{right}}, x_0(a_{\text{right}})) = -1$. The open interval $(a_{\text{left}}, a_{\text{right}})$ is the periodic window corresponding to the odd-parity sequence s . The symbol sequence changes once when a is decreased from $a = 4.0$ to a_{left} . This happens at a point a_{middle} where $\lambda_p(a_{\text{middle}}, x_0(a_{\text{middle}})) = 0$. For $a = a_{\text{middle}}$ the orbit $x(a_{\text{middle}})$ is superstable. One of the points along the orbit passes the maximum of the quadratic map, i.e. $x_k(a_{\text{middle}}) = 0.5$ for some $k = 0, 1, \dots, p-1$ and the symbol s_k flips. For even-parity sequences the condition $\lambda_p(a, x_0(a)) = 1$ defines the saddle-node bifurcation point. At this point, the continuation curve of the even-parity sequence and the continuation curve of its odd-parity saddle-node partner coincide. An example is shown in Fig. 1. The curve $(a, \lambda_p(a, x_0(a)))$ corresponding to the odd-parity sequence (001) starts at the point $(a, \lambda) = (4, -8)$. In this case $\lambda_p(a, x_0(a)) = -1$ for $a_{\text{right}} \approx 3.841499$ and $\lambda_p(a, x_0(a)) = 1$ for $a_{\text{left}} \approx 3.828427$, hence the periodic window is $(a_{\text{left}}, a_{\text{right}}) \approx (3.828427, 3.841499)$. This periodic window is depicted with vertical dashed lines in Fig. 1. The continuation curve corresponding to the even-parity sequence (011) starts at the point $(a, \lambda) = (4, 8)$. The curves corresponding to sequences (001) and (011) intersect tangentially at the saddle-node bifurcation point.

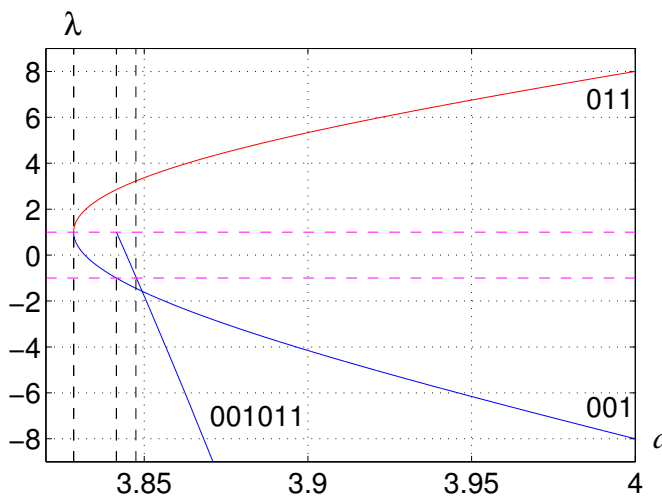


Fig. 1. The derivative λ_p versus parameter a for periodic orbits associated with symbol sequences (001) , (011) , and (001011)

Let us now describe how to identify what is the saddle-node partner of an odd-parity sequence. We start by ordering the set of symbol sequences $\Sigma = \{s = (s_0, s_1, \dots) : s_k = \pm 1\}$. We say that $s < \hat{s}$ if $s_k < \hat{s}_k$ and $\sum_{i=0}^{k-1} s_i \equiv 0 \pmod{2}$ or $s_k > \hat{s}_k$ and $\sum_{i=0}^{k-1} s_i \equiv 1 \pmod{2}$, where k is the smallest positive integer such that $s_k \neq \hat{s}_k$. This ordering of symbol sequences preserves order of points in the state space, i.e. $s(x) < s(\hat{x})$ if and only if $x < \hat{x}$. Points

belonging to a single periodic orbit have symbol sequences being cyclic permutations of a given symbol sequence, i.e. if $(x_0, x_1, \dots, x_{p-1})$ is a periodic orbit and $s(x_0) = (s_0, s_1, \dots, s_{p-1})$ then $s(x_k) = (s_k, \dots, s_{p-1}, s_0, \dots, s_{k-1})$. When the derivative $\lambda_p(a, x_0(a))$ changes sign, the last symbol of the largest cyclic permutation is changed. This is equivalent to changing the second to last symbol of the smallest cyclic permutation. For example, the order of cyclic permutations of (001) is $(001) < (010) < (100)$. It follows that at the point a_{middle} the smallest cyclic permutation $(0\underline{0}1)$ changes to $(0\underline{1}1)$ (the modified symbol is underlined). Therefore, the saddle-node partner of (001) is (011).

It is possible that the above procedure applied to a period- p sequence leads to a symbol sequence with period $p/2$. For example, cyclic permutations of (001011) are $(001011) < (011001) < (010110) < (110010) < (101100) < (100101)$. Flipping the second to last symbol in the smallest cyclic permutation $(0010\underline{1}1)$ leads to $(0010\underline{0}1)$. The resulting sequence has period 3. In such a case there is a period-doubling bifurcation at the left endpoint of the periodic window. At this point, the period- $p/2$ orbit loses stability and a stable period- p orbit is born. An example is shown in Fig. 1, where the periodic window corresponding to the sequence (001011) starts at the point where the periodic window associated with the sequence (001) ends.

From the discussion presented above it follows that periodic windows correspond to odd-parity symbol sequences. Period-doubling windows correspond to sequences s of length $p = 2k$ for which flipping the second to last symbol in the smallest cyclic permutation of s produces a symbol sequence of period k . Other odd-parity sequences correspond to saddle-node windows.

Let $W(p)$ be the number of periodic windows with period p or equivalently the number of period- p odd-parity sequences. For $p \geq 2$ all periodic windows are created either via saddle-node or period-doubling bifurcation. In each saddle-node bifurcation one of the orbits created is stable and one is unstable. For odd p there are no period-doubling windows. Hence, half of the sequences correspond to periodic windows, which means that in this case $W(p)$ is half of $P(p)$, where $P(p)$ is defined in (5). For even p there are exactly $W(p/2)$ period-doubling windows. Half of the remaining sequences correspond to periodic windows. Therefore, the formula for $W(p)$ reads

$$W(p) = \begin{cases} 2 & \text{if } p = 1, \\ 1 & \text{if } p = 2, \\ 0.5 \cdot P(p) & \text{if } p \text{ is odd, } p \geq 3, \\ 0.5 \cdot (P(p) + W(0.5 \cdot p)) & \text{if } p \text{ is even, } p \geq 4. \end{cases} \quad (6)$$

From (5) and (6) it follows that $W(p)$ grows approximately as $p^{-1}2^{p-1}$.

3. Finding Periodic Windows

In this section, we present methods to find rigorous bounds of endpoints of all low-period windows. First, we describe how to implement the interval Newton method to prove the existence of periodic orbits for one-dimensional maps.

3.1. Efficient implementation of the Newton method

Let us consider a one-dimensional continuously differentiable map $f: \mathbb{R} \mapsto \mathbb{R}$. To study period- p orbits of f we define the map $F: \mathbb{R}^p \mapsto \mathbb{R}^p$

$$[F(x)]_i = x_{(i+1) \bmod p} - f(x_i), \text{ for } i = 0, 1, \dots, p-1 \quad (7)$$

where $x = (x_0, x_1, \dots, x_{p-1})^\top$. Note that x is a zero of F if and only if x_0 is a fixed point of f^p .

The *interval Newton operator* for the map F is defined by

$$N(\mathbf{x}, \hat{x}) = \hat{x} - F'(\mathbf{x})^{-1}F(\hat{x}), \quad (8)$$

where $\mathbf{x} = (\mathbf{x}_0, \mathbf{x}_1, \dots, \mathbf{x}_{p-1})^\top$ is an interval vector and $\hat{x} \in \mathbf{x}$. The most important theorem concerning the interval Newton operator states that if $N(\mathbf{x}, \hat{x}) \subset \mathbf{x}$ then there exists a single zero of F in \mathbf{x} [Neumaier, 1990]. Hence, in order to prove the existence of a unique periodic orbit in \mathbf{x} , we choose $\hat{x} \in \mathbf{x}$, and verify that $N(\mathbf{x}, \hat{x})$ is enclosed in \mathbf{x} . Once the existence is proved, we may iterate N to narrow down the set in which the periodic orbit exists. The Jacobian

matrix of F is

$$F'(x) = \begin{pmatrix} -c_0 & 1 & 0 & \dots & 0 \\ 0 & -c_1 & 1 & \dots & 0 \\ \vdots & \vdots & \vdots & \ddots & \vdots \\ 1 & 0 & 0 & \dots & -c_{p-1} \end{pmatrix}, \quad (9)$$

where $c_k = f'(x_k)$. Below, we recall two methods to efficiently compute $F'(\mathbf{x})^{-1}F(\hat{x})$ and evaluate $\mathbf{N}(\mathbf{x}, \hat{x})$.

Theorem 1. Let $\mathbf{x} = (\mathbf{x}_0, \mathbf{x}_1, \dots, \mathbf{x}_{p-1})^\top$ be an interval vector and $\hat{\mathbf{x}} = (\hat{x}_0, \hat{x}_1, \dots, \hat{x}_{p-1})^\top$ be a point vector such that $\hat{\mathbf{x}} \in \mathbf{x}$. Assume that the intervals \mathbf{c}_k and \mathbf{g}_k are such that $f'(\mathbf{x}_k) \subset \mathbf{c}_k$ and $\hat{x}_{(k+1) \bmod p} - f(\hat{x}_k) \in \mathbf{g}_k$ for $0 \leq k < p$. If the intervals \mathbf{h}_k satisfy conditions

$$-\left(1 - \prod_{j=0}^{p-1} \mathbf{c}_j^{-1}\right)^{-1} \sum_{i=0}^{p-1} \mathbf{g}_i \prod_{j=0}^i \mathbf{c}_j^{-1} \subset \mathbf{h}_0 \quad (10a)$$

$$\mathbf{c}_k^{-1}(\mathbf{h}_{(k+1) \bmod p} - \mathbf{g}_k) \subset \mathbf{h}_k, \quad k = p-1, \dots, 2, 1. \quad (10b)$$

or

$$\left(1 - \prod_{j=0}^{p-1} \mathbf{c}_j\right)^{-1} \sum_{i=0}^{p-1} \mathbf{g}_i \prod_{j=i+1}^{p-1} \mathbf{c}_j \subset \mathbf{h}_0 \quad (11a)$$

$$\mathbf{g}_k + \mathbf{c}_k \mathbf{h}_k \subset \mathbf{h}_{k+1}, \quad k = 0, 1, \dots, p-2. \quad (11b)$$

then \mathbf{h} contains solutions of $F'(x)h = H(\hat{x})$ for all $x \in \mathbf{x}$ and $\mathbf{N}(\mathbf{x}, \hat{x}) \subset \hat{x} - \mathbf{h}$.

Formulas (10) and (11) are the backward and forward shooting versions to solve the equation $F'(x)h = F(\hat{x})$. Proof of the above result is given in [Galias, 2002] (backward shooting) and in [Galias & Garda, 2015] (forward shooting). In the backward (forward) shooting version the intervals \mathbf{h}_k are found recursively for decreasing (increasing) k . For a description of the backward shooting method see also [Coomes *et al.*, 1996]. The backward shooting method should be used when the orbit under study is unstable, because in this method multiplications by $f'(\mathbf{x}_k)^{-1}$ are carried out. Since for an unstable periodic orbit we expect that $|f'(x_k)| > 1$ for most k , then these multiplications reduce the diameter of the product and the overestimation of the result is reduced. Note that in the backward shooting version it is mildly assumed that intervals $f'(\mathbf{x}_k)$ do not contain zero. For superstable orbits with $f'(x_k) = 0$ the backward shooting version cannot be applied. In this case, and more general for stable orbits the preferred choice is the forward shooting version.

To prove the existence of a periodic orbit in the interval vector $\mathbf{x} = (\mathbf{x}_0, \mathbf{x}_1, \dots, \mathbf{x}_{p-1})^\top$ one computes $\mathbf{c}_k = f'(\mathbf{x}_k)$ and $\mathbf{g}_k = \hat{x}_{(k+1) \bmod p} - f(\hat{x}_k)$ in interval arithmetic. Then, depending on the version one computes \mathbf{h}_0 as the interval evaluation of the left hand side of inclusions (10a) or (11a) and the remaining \mathbf{h}_k using the left hand side of inclusions (10b) or (11b). Finally, if $\hat{x} - \mathbf{h} \subset \mathbf{x}$ then the existence of a single periodic orbit belonging to \mathbf{x} is confirmed. Formulas (10) and (11) may also be used for efficient evaluation of standard (non-interval) Newton method.

3.2. Finding periodic windows endpoints

To find periodic windows we use the continuation method starting at the parameter value $a = 4.0$ for which positions of periodic orbits are known (see Sec. 2). Let us briefly recall this method (for more details see [Galias & Garda, 2015]).

We move in the parameter space from $a = 4$ decreasing a and updating the position of the corresponding periodic orbit until the orbit becomes stable. In each continuation step we select $\Delta a > 0$ and assign test value $a_{\text{test}} = a - \Delta a$. Next, we iteratively apply the (real) Newton operator to improve the approximation $x(a_{\text{test}})$ of the position of the periodic orbit for the test value. To speed up computations we use a shooting method to evaluate the Newton operator. If the Newton method converges to a periodic point with a correct symbol sequence (as explained in Sec. 2 the symbol sequence changes only once along the continuation curve) we accept the test point (we set $a = a_{\text{test}}$), increase Δa , and try the next test point. In the opposite case the test point is rejected, Δa is decreased, and the above procedure is repeated. Continuation is carried out until the bifurcation point where λ_p reaches 1. In case

of odd-parity sequences, the continuation method produces two points, which are close to window's right and left endpoints.

As an initial point for the Newton method we use $x(a_{\text{test}}) = x(a) - \Delta a \cdot \partial x / \partial a$, where $x(a)$ is the position of the orbit for the current parameter value a and $\partial x / \partial a = (\partial x_0 / \partial a, \partial x_1 / \partial a, \dots, \partial x_{p-1} / \partial a)^\top$ is the derivative of the position of the periodic orbit with respect to a (compare [Galias & Tucker, 2014]). The derivative $\partial x / \partial a$ is found using the implicit function theorem applied to the map $F: \mathbb{R}^{p+1} \mapsto \mathbb{R}^p$ defined by $[F(x_0, x_1, \dots, x_{p-1}, a)]_i = x_{(i+1) \bmod p} - f_a(x_i)$. $\partial x / \partial a$ is the solution of the linear equation $\partial F / \partial x \cdot \partial x / \partial a + \partial F / \partial a = 0$, where $[\partial F / \partial a]_k = -x_k(1 + x_k)$, and the matrix $\partial F / \partial x$ has the form (9). To efficiently find the solution $\partial x / \partial a$ one should use a shooting method.

3.3. Finding rigorous bounds of periodic window's endpoints

In this section, we describe how to find rigorous bounds of periodic windows' endpoints. We assume that we have two points on the continuation curve, which are close to window's endpoints. We start by computing an accurate estimate \tilde{a}_{right} of the right endpoint of the window. This can be done using the bisection method or the Newton method to solve the equation $\lambda_p(a, x_0(a)) = -1$. The latter approach is faster. Next, we select $\underline{a}_{\text{right}} < \tilde{a}_{\text{right}} < \bar{a}_{\text{right}}$ and using Theorem 1 we evaluate the interval Newton operator to prove the existence of periodic orbits for $\underline{a}_{\text{right}}$ and \bar{a}_{right} with proper stability, i.e. $\lambda_p(\underline{a}_{\text{right}}, x_0(\underline{a}_{\text{right}})) > -1 > \lambda_p(\bar{a}_{\text{right}}, x_0(\bar{a}_{\text{right}}))$. The interval $[\underline{a}_{\text{right}}, \bar{a}_{\text{right}}]$ contains the true periodic window's right endpoint.

The upper bound of the left endpoint a_{left} is obtained by finding \bar{a}_{left} for which $\lambda_p(\bar{a}_{\text{left}}, x_0(\bar{a}_{\text{left}}))$ is smaller than and close to 1. Using the interval Newton operator we prove the existence of a stable periodic orbit for \bar{a}_{left} . Rigorous lower bound of a_{left} is found using a method depending on the window's type. For period-doubling windows one may use a lower bound of the right endpoint of the periodic window which is the period-doubling parent of the considered window.

For saddle-node windows the procedure is more complicated. Note that when a converges to the bifurcation value derivatives $\partial x / \partial a$ go to infinity. In consequence, the parameter continuation method described in the previous section cannot pass the saddle-node bifurcation point. One possible solution is to exchange the role of the continuation parameter and one of the variables. In this approach instead of changing parameter a we modify the value of a selected variable (for example x_0). Another possibility is to use a more general pseudo-arc length continuation, where the continuation direction is chosen automatically. We select the former method because it is simpler to implement and is sufficient for our purpose. In each continuation step, we consider a test value $x_0 = x_{0,\text{test}}$ and solve the equation $G(y) = 0$, where $y = (a, x_1, x_2, \dots, x_{p-1})^\top$, $[G(y)]_i = x_{(i+1) \bmod p} - ax_i(1 - x_i)$, and x_0 is fixed. Implementation of the Newton method for the map G requires solving the equation

$$\begin{pmatrix} -b_0 & 1 & 0 & \dots & 0 & 0 \\ -b_1 & -c_1 & 1 & \dots & 0 & 0 \\ \vdots & \vdots & \vdots & \ddots & \vdots & \vdots \\ -b_{p-2} & 0 & 0 & \dots & -c_{p-2} & 1 \\ -b_{p-1} & 0 & 0 & \dots & 0 & -c_{p-1} \end{pmatrix} \begin{pmatrix} h_0 \\ h_1 \\ \vdots \\ h_{p-2} \\ h_{p-1} \end{pmatrix} = \begin{pmatrix} g_0 \\ g_1 \\ \vdots \\ g_{p-2} \\ g_{p-1} \end{pmatrix}, \quad (12)$$

where $b_k = x_k(1 - x_k)$, $c_k = f'_a(x_k) = a(1 - 2x_k)$, $g_k = x_{(k+1) \bmod p} - ax_k(1 - x_k)$. The forward shooting method to solve the above equation is

$$h_0 = - \left(\sum_{k=0}^{p-1} b_k \prod_{j=k+1}^{p-1} c_j \right)^{-1} \sum_{k=0}^{p-1} g_k \prod_{j=k+1}^{p-1} c_j, \quad (13a)$$

$$h_1 = g_0 + b_0 h_0, \quad (13b)$$

$$h_k = g_{k-1} + b_{k-1} h_0 + c_{k-1} h_{k-1}, \quad k = 2, 3, \dots, p-1. \quad (13c)$$

Equations (13) can also be used for efficient evaluation of the interval Newton operator for the map G .

The variable continuation method described above allows us to obtain a very good approximation of the saddle-node bifurcation point $(a, \lambda) = (a_{\text{left}}, 1)$. To obtain rigorous bounds for a_{left} we start by finding two points (\hat{a}, \hat{x}_0) and (\tilde{a}, \tilde{x}_0) lying on the continuation curve close to the bifurcation point such that $\lambda_p(\hat{a}, \hat{x}_0) < 1 < \lambda_p(\tilde{a}, \tilde{x}_0)$. Using the interval Newton method applied to G we prove the existence of periodic orbits with proper stability (one stable, one

unstable) for these two points. Next, we create a candidate interval vector $\bar{\mathbf{a}}_{\text{left}} \times \mathbf{x}_0$ satisfying conditions $\hat{x}_0, \tilde{x}_0 \in \mathbf{x}_0$ and $\hat{a}, \tilde{a} \in \bar{\mathbf{a}}_{\text{left}} = [\underline{a}_{\text{left}}, \bar{a}_{\text{left}}]$. We apply the interval Newton operator to prove the existence of a periodic orbit for each x_0 belonging to the candidate set. Finally, we compute the derivative $\partial^2 a / \partial x_0^2$ over the candidate set and verify that it does not contain 0. It follows that the candidate set contains the saddle-node bifurcation point and in consequence $\underline{a}_{\text{left}}$ and \bar{a}_{left} are bounds for the periodic window's left endpoint.

3.4. Interval Newton method to find bifurcation points

An alternative approach to find bounds for periodic window's endpoints is to apply the interval Newton method to prove the existence of bifurcation points. To study bifurcation points let us consider the map $H_{\lambda_0}: \mathbb{R}^{p+1} \mapsto \mathbb{R}^{p+1}$ defined by $[H_{\lambda_0}(z)]_i = x_{(i+1) \bmod p} - ax_i(1-x_i)$ for $i = 0, 1, 2, \dots, p-1$ and $[H_{\lambda_0}(z)]_p = a^p(1-2x_{p-1}) \cdots (1-2x_1)(1-2x_0) - \lambda_0$, where $z = (x_0, x_1, \dots, x_{p-1}, a)^\top$ and $\lambda_0 = \pm 1$. Zeros of H_{λ_0} correspond to bifurcations of period- p orbits. The first p components of H_{λ_0} provide periodic point conditions, while the last component ensures that the derivative $\lambda_p(a, x_0)$ is equal to λ_0 . $\lambda_0 = -1$ and $\lambda_0 = 1$ will be used to study period-doubling and saddle-node bifurcation points, respectively. The Jacobian matrix of H_{λ_0} has the form

$$H'_{\lambda_0}(x) = \begin{pmatrix} -c_0 & 1 & 0 & \dots & 0 & -b_0 \\ 0 & -c_1 & 1 & \dots & 0 & -b_1 \\ \vdots & \vdots & \vdots & \ddots & \vdots & \vdots \\ 1 & 0 & 0 & \dots & -c_{p-1} & -b_{p-1} \\ -2ad_0 & -2ad_1 & -2ad_2 & \dots & -2ad_{p-1} & pa^{-1}w_{p-1} \end{pmatrix}, \quad (14)$$

where $b_k = x_k(1-x_k)$, $c_k = f'_a(x_k) = a(1-2x_k)$, $w_k = \prod_{i=0}^k c_i$, $d_k = \prod_{i=0, i \neq k}^{p-1} c_i$.

To prove that the interval vector \mathbf{z} contains a bifurcation point we need to show that $N(\mathbf{z}, \hat{z}) = \hat{z} - H'_{\lambda_0}(\mathbf{z})^{-1}H_{\lambda_0}(\hat{z}) \subset \mathbf{z}$ where $\hat{z} \in \mathbf{z}$. Efficient evaluation of the interval Newton operator for the map H_{λ_0} is more involving than for the map F . Below, we present a forward shooting method to compute the interval vector \mathbf{h} containing solutions of $H'_{\lambda_0}(z)h = H_{\lambda_0}(\hat{z})$ for $z \in \mathbf{z}$.

Theorem 2. Let $\mathbf{z} = (\mathbf{x}_0, \mathbf{x}_1, \dots, \mathbf{x}_{p-1}, \mathbf{a})^\top$ be an interval vector and $\hat{z} = (\hat{x}_0, \hat{x}_1, \dots, \hat{x}_{p-1}, \hat{a})^\top \in \mathbf{z}$. Assume that

$$\mathbf{a}(1-2\mathbf{x}_k) \subset \mathbf{c}_k, \quad \mathbf{x}_k(1-\mathbf{x}_k) \subset \mathbf{b}_k, \quad \hat{x}_{(k+1) \bmod p} - \hat{a}\hat{x}_k(1-\hat{x}_k) \in \mathbf{g}_k, \quad (15a)$$

$$\prod_{i=0, i \neq k}^{p-1} \mathbf{c}_i \subset \mathbf{d}_k, \quad \prod_{i=0}^{p-1} \hat{a}(1-2\hat{x}_i) \in \mathbf{e}, \quad \sum_{j=0}^k \mathbf{b}_j \prod_{i=j+1}^k \mathbf{c}_i \subset \mathbf{u}_k, \quad \sum_{j=0}^k \mathbf{g}_j \prod_{i=j+1}^k \mathbf{c}_i \subset \mathbf{v}_k, \quad \prod_{i=0}^k \mathbf{c}_i \subset \mathbf{w}_k, \quad (15b)$$

$$2\mathbf{a}\left(\mathbf{d}_0 + \sum_{i=1}^{p-1} \mathbf{d}_i \mathbf{w}_{i-1}\right) \subset \mathbf{q}_0, \quad 2\mathbf{a} \sum_{i=1}^{p-1} \mathbf{d}_i \mathbf{u}_{i-1} - \frac{p\mathbf{w}_{p-1}}{\mathbf{a}} \subset \mathbf{q}_1, \quad \lambda_0 + \mathbf{e} - 2\mathbf{a} \sum_{i=1}^{p-1} \mathbf{d}_i \mathbf{v}_{i-1} \subset \mathbf{r}, \quad (15c)$$

for $0 \leq k < p$. If intervals \mathbf{h}_k satisfy conditions

$$\frac{\mathbf{r}\mathbf{u}_{p-1} + \mathbf{v}_{p-1}\mathbf{q}_1}{\mathbf{q}_0\mathbf{u}_{p-1} + (1-\mathbf{w}_{p-1})\mathbf{q}_1} \subset \mathbf{h}_0, \quad \frac{-\mathbf{q}_0\mathbf{v}_{p-1} + (1-\mathbf{w}_{p-1})\mathbf{r}}{\mathbf{q}_0\mathbf{u}_{p-1} + (1-\mathbf{w}_{p-1})\mathbf{q}_1} \subset \mathbf{h}_p \quad (16a)$$

$$\mathbf{v}_k + \mathbf{w}_k \mathbf{h}_0 + \mathbf{u}_k \mathbf{h}_p \subset \mathbf{h}_{k+1}, \quad k = 0, 1, \dots, p-2. \quad (16b)$$

then \mathbf{h} contains solutions of $H'_{\lambda_0}(z)h = H_{\lambda_0}(\hat{z})$ for all $z \in \mathbf{z}$ and $N(\mathbf{z}, \hat{z}) \subset \hat{z} - \mathbf{h}$.

Proof. Using definitions $b_k = x_k(1-x_k)$, $c_k = a(1-2x_k)$ and $g_k = \hat{x}_{(k+1) \bmod p} - \hat{a}\hat{x}_k(1-\hat{x}_k)$, the first p equations in $H'_{\lambda_0}(z)h = H_{\lambda_0}(\hat{z})$ can be written as $h_{(k+1) \bmod p} = g_k + c_k h_k + b_k h_p$ for $k = 0, 1, \dots, p-1$. Substituting recursively h_k from the k th equation into the $(k+1)$ th equation yields

$$h_{(k+1) \bmod p} = v_k + w_k h_0 + u_k h_p, \quad k = 0, 1, \dots, p-1, \quad (17)$$

where $u_k = \sum_{j=0}^k b_j \prod_{i=j+1}^k c_i$, $v_k = \sum_{j=0}^k g_j \prod_{i=j+1}^k c_i$, and $w_k = \prod_{i=0}^k c_i$. The last equation in $H'_{\lambda_0}(z)h = H_{\lambda_0}(\hat{z})$ can be written as $-2a \sum_{i=0}^{p-1} d_i h_i + p w_{p-1} h_p/a = e - \lambda_0$, where $d_k = \prod_{i=0, i \neq k}^{p-1} c_i$ and $e = \prod_{i=0}^{p-1} \hat{a}(1-2\hat{x}_i)$. Eliminating h_1 ,

h_2, \dots, h_{p-1} from the last equation we obtain

$$2a \left(d_0 + \sum_{i=1}^{p-1} d_i w_{i-1} \right) h_0 + \left(2a \sum_{i=1}^{p-1} d_i u_{i-1} - \frac{p w_{p-1}}{a} \right) h_p = \lambda_0 + e - 2a \sum_{i=1}^{p-1} d_i v_{i-1}. \quad (18)$$

Solving (17) with $k = p - 1$ and (18) yields

$$h_0 = \frac{r u_{p-1} + v_{p-1} q_1}{q_0 u_{p-1} + (1 - w_{p-1}) q_1}, \quad h_p = \frac{-q_0 v_{p-1} + (1 - w_{p-1}) r}{q_0 u_{p-1} + (1 - w_{p-1}) q_1}, \quad (19)$$

where $q_0 = 2a(d_0 + \sum_{i=1}^{p-1} d_i w_{i-1})$, $q_1 = 2a \sum_{i=1}^{p-1} d_i u_{i-1} - p w_{p-1} a^{-1}$, $r = \lambda_0 + e - 2a \sum_{i=1}^{p-1} d_i v_{i-1}$. We have shown that h_0, h_p defined in (19) and h_1, h_2, \dots, h_{p-1} defined in (17) are the solutions of $H'_{\lambda_0}(z)h = H_{\lambda_0}(\hat{z})$. It follows that intervals \mathbf{h}_k satisfying conditions (16) enclose all solutions of $H'_{\lambda_0}(z)h = H_{\lambda_0}(\hat{z})$ for $z \in \mathbf{z}$. ■

In practice, to evaluate the interval Newton operator we compute intervals $\mathbf{c}_k, \mathbf{b}_k, \mathbf{g}_k, \mathbf{d}_k, \mathbf{e}, \mathbf{u}_k, \mathbf{v}_k, \mathbf{w}_k, \mathbf{q}_0, \mathbf{q}_1, \mathbf{r}$, and \mathbf{h}_k in interval arithmetic using left hand sides of inclusions (15) and (16). From the inclusion property of interval computations it follows that the corresponding inclusions are automatically satisfied.

Let us note that the method to evaluate the interval Newton method for the map H_{λ_0} formulated in Theorem 2 can be implemented to have a linear complexity versus p both in time and memory. To ensure this property we have to use recursive formulas for the evaluation of \mathbf{u}_k and \mathbf{v}_k , for example $\mathbf{u}_0 = \mathbf{b}_0$, $\mathbf{u}_k = \mathbf{b}_k + \mathbf{c}_k \mathbf{u}_{k-1}$, $k = 1, 2, \dots, p - 1$.

To find bounds of the right endpoints of a periodic window we construct the interval vector \mathbf{z} containing the bifurcation point candidate \hat{z} and prove that $N(\mathbf{z}, \hat{z}) \subset \mathbf{z}$ for the map H_{λ_0} with $\lambda_0 = -1$. For saddle-node periodic window to find bounds of left endpoints we consider the map H_{λ_0} with $\lambda_0 = 1$. This method does not work for left endpoints of period-doubling windows because in this case at the bifurcation point two solution curves corresponding to the period-doubling window and its parent intersect and in consequence the matrix $H'_{\lambda_0}(z)$ is not invertible. In this case bounds for the left endpoint are found as bounds for the right endpoint of the parent.

The map H_{λ_0} provides an alternative approach to find approximate position of periodic windows' endpoints. To find the window's right endpoint we use the (non-interval) Newton method applied to the map H_{λ_0} with $\lambda_0 = -1$ with the starting point $a = 4$ and $(x_k(4.0))_{k=0}^{p-1}$ being the position of the periodic orbit for $a = 4$. If the Newton method does not converge we may use the modified Newton method [Stoer & Bulirsch, 2002], where the step size is decreased in case of a failure. Provided that the method converges to the periodic window's right endpoint we apply the Newton method for the map H_{λ_0} with $\lambda_0 = 1$ and with the initial point being the right endpoint to find the window's left endpoint. It will be shown in Sec. 4 that this method is much faster than the continuation based approach.

3.5. Locating all periodic windows with a given period

To find all period- p windows, we have to apply methods presented in previous sections to $W(p)$ period- p sequences $s = (s_0, s_1, \dots, s_{p-1})$ with $s_k \in \{0, 1\}$. The total number of sequences of length p is 2^p . It is sufficient to consider odd-parity sequences only (even-parity sequences produce unstable branches of continuation curves, see Sec. 2). Sequences with the period smaller than p should be skipped (they correspond to periodic orbits with the period being a proper divisor of p). Out of the p sequences corresponding to the same cycle it is sufficient to choose only one (the other produce other points belonging to the same periodic orbit). It follows that approximately $2^{p-1}/p$ sequences are to be considered.

For each sequence $s = (s_0, s_1, \dots, s_{p-1})$ we find the position of the period- p point of the tent map using (4) and the position of the period- p point of $f_{4,0}$ using (3). Next, we find approximations of the endpoints of the periodic window. As described in Secs. 3.2 and 3.4, we may use the continuation method or the Newton method applied to the map H_{λ_0} .

Finally, we find rigorous bounds for window endpoints. This is carried out using method described in Secs. 3.3 or 3.4. To ensure that the proper endpoint has been found we verify whether the symbol sequence of the periodic orbit at bifurcation points agrees with symbol sequence considered. For the right endpoint the sequence should be equal to the starting sequence s , while for the left endpoint there should be one symbol at a given position flipped when compared to s .

In this way for each period- p window we find rigorous bounds $[\underline{a}_{\text{left}}, \bar{a}_{\text{left}}]$ and $[\underline{a}_{\text{right}}, \bar{a}_{\text{right}}]$ of its left and right endpoints and bounds of its width can be computed as $[\underline{w}, \bar{w}] = [\underline{a}_{\text{right}} - \bar{a}_{\text{left}}, \bar{a}_{\text{right}} - \underline{a}_{\text{left}}]$.

4. Numerical Study of Periodic Windows

In this section, we carry out rigorous numerical study of low-period windows using methods presented in previous sections. Let us first compare the performance of two techniques to find all low-period windows: the continuation based approach to find periodic windows combined with the bisection technique to find rigorous bounds of windows' endpoints (see Secs. 3.2 and 3.3) and the direct Newton method based approach to find bifurcation points and prove their existence (see Sec. 3.4).

The test problem is to find all periodic windows with periods $2 \leq p \leq 20$. The computation software uses the CAPD library [CAPD] for interval arithmetic computations and the MPFR library [MPFR] for multiple precision support. For the test problem the total computation time using a single core 3.1 GHz processor is 3.25 hours for the first method and 355 seconds for the second method. The main reason for longer computations in case of the first method is that in the continuation algorithm the Newton method is used to improve approximations of positions of periodic orbits for many test points, while in the second approach the Newton method is used directly to find bifurcation points. Another advantage of the second method is that it produces more accurate bounds for positions of periodic windows in shorter time. The diameter of the interval containing the true total width $\mu(\bigcup_{p=2}^{20} \mathcal{S}_{\text{periodic},p})$ is $1.22 \cdot 10^{-34}$ for the first method and $1.42 \cdot 10^{-71}$ for the second method. The lower accuracy for the first method is caused by stopping the bisection method at the threshold $\Delta a < 10^{-40}$. Better accuracy could be achieved using a smaller threshold at the cost of further increase of computation times. Results of these computations show that the second method offers much better performance both in terms of speed and accuracy. It appears that finding bifurcation points, which are solutions of $H_{\lambda_0}(z) = 0$ for $\lambda_0 = -1$ and then for $\lambda_0 = 1$ from the initial point $a = 4$ is a relatively easy numerical problem. The conclusion is that, if possible, one should use the direct Newton method offering quadratic convergence, instead of the more robust but slower continuation based method.

4.1. All periodic windows with period $p \leq 32$

The algorithm presented in Section 3.5 has been applied to find periodic windows with periods $p \leq 32$. In all cases, apart from a single symbol sequence of length 30, the direct Newton method to find bifurcation points was used. The sequence, for which the direct Newton method failed, was processed using the continuation based method.

The results are presented in Table 1. We report the number $W(p)$ of periodic windows and the number $W_{\text{PD}}(p)$ of period-doubling windows with period p , an enclosure of the total width $\mu_p = \mu(\mathcal{S}_{\text{periodic},p})$ of period- p windows. Computations have been carried out using multiple precision interval arithmetic with 256 bits. Such accuracy makes it possible to obtain very accurate approximations of periodic windows' endpoints and widths. We have shown that the measure of the set $\bigcup_{p=2}^{32} \mathcal{S}_{\text{periodic},p}$ belongs to the interval $0.6115900138996778632303125786785586609384609657336077644714442490591_0^7$ with the diameter equal to $6 \cdot 10^{-68}$. The results presented in Table 1 are given with a lower precision for the sake of brevity. It is interesting to note that computations in standard double precision interval arithmetic do not detect all periodic windows for periods $p \geq 13$ (compare [Galias & Garda, 2015]).

The number of periodic windows reported in [Tucker & Wilczak, 2009] is smaller than the true number of periodic windows already for $p \geq 13$. Out of the total number of 67108864 periodic windows with periods $2 \leq p \leq 32$ only 482967 were found in [Tucker & Wilczak, 2009]. This is a consequence of using a criterion to stop the search for very narrow intervals. The total width of periodic windows with period $2 \leq p \leq 32$ is larger than the lower bound reported in [Tucker & Wilczak, 2009] by only $9.47 \cdot 10^{-7}$ in spite of the fact that very few windows were found when compared to the total number of windows. This means that the approach used in [Tucker & Wilczak, 2009] is successful in finding a good lower bound of the measure of the set $\mathcal{S}_{\text{periodic}}$.

The total widths μ_p of period- p windows is plotted in Fig. 2. Note that μ_p generally decreases with p , however for even $p = 2k \geq 4$ we have $\mu_{2k} > \mu_{2k-1}$. This phenomenon is related to the existence of period-doubling windows and will be discussed in the following section. Also note that values of μ_p for prime $p > 2$ are positioned along an almost straight line while μ_p for composite p are well above this line. We will give some explanations of this phenomenon in the following section.

Table 1. The number $W(p)$ of periodic windows found and their total width μ_p

p	$W(p)$	$W_{PD}(p)$	μ_p	$\mu_{p,PD}/\mu_p$
2	1	1	0.44948974278317809819 ₇ ⁸	1.0000
3	1	0	0.01307188279731774870 ₇ ⁸	0
4	2	1	0.09526738648543799923 ₅ ⁶	0.99301
5	3	0	0.00352281749623828628 ₈ ⁹	0
6	5	1	0.01005352567729128192 ₇ ⁸	0.60792
7	9	0	0.00097010870578457644 ₄ ⁵	0
8	16	2	0.02119916441295792315 ₉ ⁰	0.97395
9	28	0	0.00052448546164507295 ₈ ⁹	0
10	51	3	0.00270572410469467575 ₅ ⁶	0.64132
11	93	0	0.00012152861481443824 ₆ ⁷	0
12	170	5	0.00417709984321127417 ₅ ⁶	0.78424
13	315	0	0.00004417992847124171 ₀ ¹	0
14	585	9	0.00074534105321868369 ₃ ²	0.64919
15	1091	0	0.0001386641149201338 ₂₉ ³⁰	0
16	2048	16	0.00484465053309528382 ₇ ⁸	0.97108
17	3855	0	0.0000097305449095335 ₆₉ ⁷⁰	0
18	7280	28	0.00045930680596697579 ₈ ⁷	0.55496
19	13797	0	0.00000462588850026189 ₉ ⁸	0
20	26214	51	0.00110324381331917788 ₃ ⁴	0.80373
21	49929	0	0.00003586831940909627 ₆ ⁷	0
22	95325	93	0.00009303393392834776 ₄ ⁵	0.65315
23	182361	0	0.0000125592016972887 ₆ ⁷	0
24	349520	170	0.00138360468318981486 ₁ ⁰	0.84357
25	671088	0	0.00001723245763604226 ₃ ⁴	0
26	1290555	315	0.0000381591261175345 ₅ ⁶	0.65323
27	2485504	0	0.00001473183154822258 ₆ ⁷	0
28	4793490	585	0.00030281063533019706 ₃ ²	0.80769
29	9256395	0	0.00000029326056197972 ₆ ⁵	0
30	17895679	1091	0.00013907841369244839 ₈ ⁷	0.48146
31	34636833	0	0.00000013466473698890 ₆ ⁵	0
32	67108864	2048	0.0011494480189057576 ₆ ⁵	0.97206
138871108		4419	0.61159001389967786323 ₀ ¹	0.95625

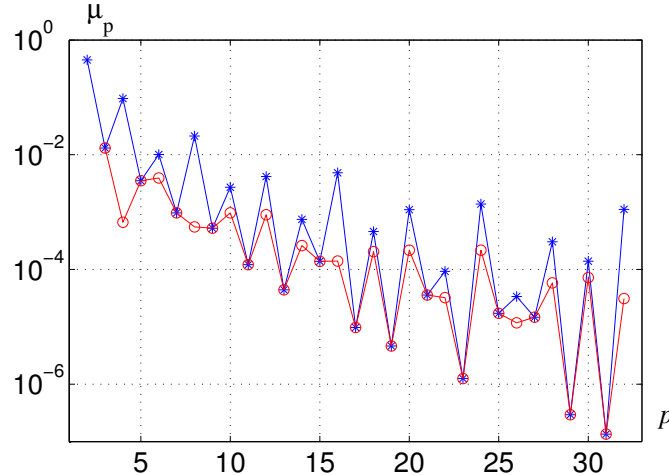


Fig. 2. The total widths $\mu_p = \mu(S_{\text{periodic},p})$ of period- p windows (the “*” symbol) and the total width of period- p saddle-node windows (the “○” symbol)

4.2. Properties of periodic windows

In this section we discuss properties of low-period windows. Widths of periodic windows versus p are plotted in Fig. 3. The minimum width decreases exponentially with p . Observe that for $p = 13$ the minimum width is close to the double precision machine epsilon. This explains why some periodic windows with periods $p \geq 13$ are not detected when the double precision arithmetic is used. Period-doubling windows are depicted using a different color. Note that they occupy the upper part of the plot. For even p , period-doubling windows have the dominating influence on the total width μ_p . In the last column of Table 1, we present the ratios $\mu_{p,\text{PD}}/\mu_p$, where $\mu_{p,\text{PD}}$ is the total width of period-doubling windows with period p . One can see that these ratios are above 0.48 for all even p , and are close to 1.0 for p being powers of 2. The ratio $\mu_{2-32,\text{PD}}/\mu_{2-32}$ of the total width of all period-doubling windows and all periodic windows with $2 \leq p \leq 32$ is 0.95625 (cf. Table 1). This is mainly due to the widest period-doubling cascade (the period-2 window and its descendants), with the width of 0.5696916 (93% of the total width 0.61159). If we neglect the first period-doubling cascade, then the total width of period-doubling windows constitutes 36% of the width of all periodic windows. This is an important contribution, especially if take into account the fact that there are less than 5000 period-doubling windows and more than $1.3 \cdot 10^8$ saddle-node windows with periods $p \leq 32$.

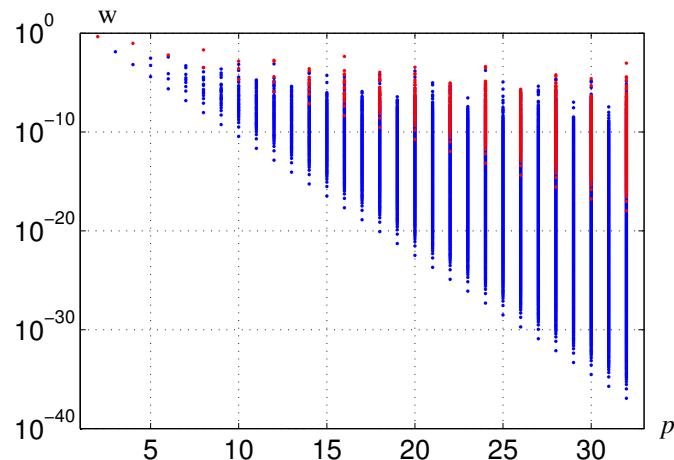
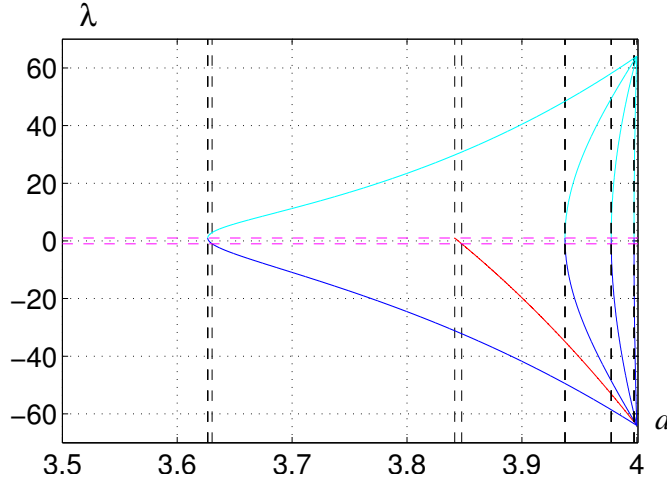
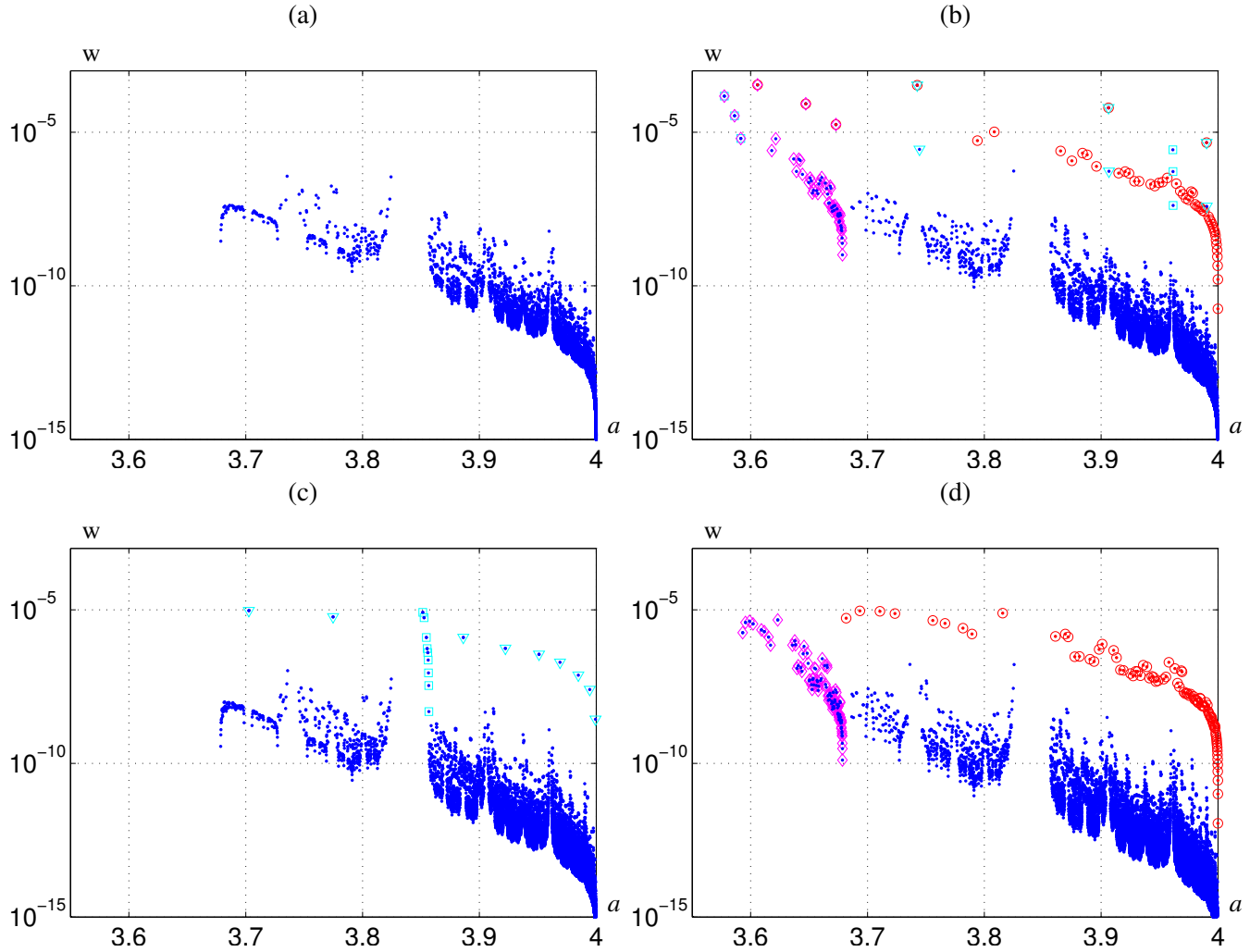


Fig. 3. Widths of periodic windows versus period

To explain the large contribution of period-doubling windows, in Fig. 4 we plot derivatives $\lambda_p(a, x_0(a))$ for period-6 orbits versus a . Results for odd-parity sequences leading to period-doubling and saddle-node windows are plotted using red and blue colors, respectively. Results for even-parity saddle-node partners of odd-parity sequences are plotted using cyan color. First, let us note that windows existing for larger a are narrower. This is due to the fact that continuation curves for odd-parity sequences start at the same point $(a, \lambda) = (4.0, -2^p)$ and their slope depends on the value at which they intersect the line $\lambda = 1$. The main difference between period-doubling and saddle-node windows windows is that for saddle-node windows the curve $\lambda(a)$ is tangent to the vertical line at the left endpoint of the window, while for the period-doubling windows the derivative $\lambda'(a)$ is finite over the whole window. In consequence, saddle-node windows are narrower. In the example shown in Fig. 4 the width of the period-doubling window is larger than widths of all saddle-node windows. This happens in spite of the fact that the widest saddle-node window exists for much smaller a .

Below, we try to explain why the total width of period- p windows strongly depends on factorization of p . Plots of periodic windows' widths versus a for periodic windows with $p = 19, 20, 21, 22$ are shown in Fig. 5. One can see that generally widths of periodic windows decrease when a grows. The windows' widths drop below 10^{-15} for a very close to 4.0. Results for saddle node and period-doubling windows are plotted using the blue and red dots, respectively. Additionally, period-doubling windows are depicted using the circle symbol, and selected saddle-node windows are depicted using other symbols (squares, diamonds, and triangles). As it will be explained later, they correspond to period-tupling symbol sequences obtained by concatenation of shorter sequences (compare also [Derrida *et al.*, 1978; Wan-Zhen *et al.*, 1984]).

Note that period-doubling windows, in general, have widths which are several orders of magnitude larger than

Fig. 4. Derivatives λ_p for period-8 orbits versus a Fig. 5. Periodic windows' widths versus a for period-19 windows (a), period-20 windows (b), period-21 windows (c), and period-22 windows (d)

widths of saddle-node windows for similar values of a . In a sense, periodic windows inherit width from their parents, and in consequence their width is much larger than the width of saddle-node windows with the same period and

a similar value of a (cf. Fig. 4 and the discussion in the text). This explains why $\mu_{2k} > \mu_{2k-1}$ (cf. Fig. 3 and Table 1).

However, we still need to explain why for odd and composite p the total width is larger than for prime p . Let us note that parts of the plots concerning saddle-node windows depicted with dots only are similar, especially for p of the same parity (compare Fig. 5(a) with (c) and (b) with (d)). For $p = 19$, which is a prime number, there are no results outside this part of the plot. For $p = 20$ and $p = 22$ there are 51 and 93 period-doubling windows, respectively. Let us note that for $p = 21$ there exist windows forming a similar structure as period-doubling windows for $p = 20$ and $p = 22$. To explain this phenomenon let us recall how the period-doubling sequences emerge from their parents. Let us assume that $u = (u_0, u_1, \dots, u_{k-1})$ is an odd-parity sequence and that u is the smallest cyclic permutation of u . Period-doubling sequence s of length $p = 2k$ is created from u by concatenating u and $v = (u_0, u_1, \dots, u_{k-3}, 1 - u_{k-2}, u_{k-1})$, which is obtained from u by flipping the second to last symbol, i.e. $s = (u, v)$. Note that since u is odd-parity and v is even-parity, the resulting sequence is of odd parity. In a similar way, we may obtain sequences of length $p = lk$ from u by concatenating l_1 copies of u and $l - l_1$ copies of v , where l_1 is odd to preserve the odd-parity of the final sequence. This process is called period l -tupling. For example, when $p = 3k$ period-tripling of u produces the sequence $s = (u, v, v)$. Period-quadrupling with $p = 4k$ gives two choices: $s = (u, v, v, v)$ and $s = (u, u, u, v)$, while for $p = 5k$ there are three possibilities: $s = (u, v, v, v, v)$, $s = (u, u, u, v, v)$, and $s = (u, u, v, u, v)$.

Let us now consider $p = 21$. There are nine periodic windows with period $k = 7$. Each of them produces a single period-21 odd-parity sequence via period-tripling. Periodic windows corresponding to the resulting period-21 sequences are plotted in Fig. 5(c) using triangle symbols. In each case, the period- p window lies close to the corresponding period- k window. For example, the sequence $u = (0111101)$ with the periodic window $(a_{\text{left}}, a_{\text{right}}) \approx (3.7016408, 3.7021549)$ leads to $s = (0111101 0111111 0111111)$ with the periodic window $(a_{\text{left}}, a_{\text{right}}) \approx (3.7026674, 3.7026768)$. Period-21 sequences can also be obtained by concatenating period-3 sequences. There is one odd-parity period-3 sequence $u = (001)$. From it, via period-septupling one can obtain the following nine period-21 sequences: (u, v, u, u, u, u, v) , (u, v, u, u, v, u, u) , (u, v, v, u, v, u, v) , (u, v, v, u, u, u, u) , (u, v, v, u, u, v, v) , (u, v, v, v, u, v, u) , (u, v, v, v, u, u, v) , (u, v, v, v, v, v, v) , where $v = (011)$. Periodic windows corresponding to these sequences are plotted in Fig. 5(c) using square symbols. Since all sequences are created from the same period-3 sequence, the corresponding periodic windows are located close to each other in the parameter space.

Let us now go back to the case $p = 22$. There are 93 period-doubling windows for $p = 22$ obtained from odd-parity period-11 sequences. Period-22 sequences can also be obtained by concatenating period-2 sequences. There is one period-2 odd-parity sequence: $u = (01)$. From it, via period 11-tupling one can create 93 period-22 odd-parity sequences. Periodic windows corresponding to these sequences are plotted in Fig. 5(d) using diamond symbols.

The case $p = 20$ is more complex because $p = 20$ has more divisors. Similarly as for $p = 22$, there are period-doubling windows and sequences created from $u = (01)$. For $p = 20$, there are 53 period-doubling windows denoted with the circle symbol and 53 period 10-tupling windows created from $u = (01)$ denoted using diamond symbols in Fig. 5(b). Other divisors of 20 are 4 and 5. There are two period-4 odd-parity sequences: $u' = (0001)$ and $u'' = (0111)$. Each of them produces three period-20 sequences via period-quintupling: $s = (u, v, v, v, v)$, $s = (u, u, u, v, v)$, and $s = (u, u, v, u, v)$. These sequences are denoted using square symbols in Fig. 5(b). Sequences created from $u' = (0001)$ exist for a close to 3.9615, while sequences created from $u'' = (0111)$ exist for $a < 3.6$. Note that these three sequences can be also created from the sequence (01) via period 11-tupling, and hence are also denoted using diamond symbols. There are three period-5 odd-parity sequences: (00001) , (00111) , and (01101) . Each of them produces two period-20 sequences via period-quadrupling: (u, v, u, u) and (u, v, v, v) . These sequences are denoted using triangle symbols in Fig. 5(b). Sequences of the type (u, v, u, u) are also period-doubling sequences and hence in Fig. 5(b) they are denoted also using circle symbols.

Period-doubling and more generally period-tupling sequences are observed for composite periods. As one can see in Fig. 5 widths of period-tupling sequences are in general larger than widths of other sequences. This explains why for periods being composite numbers the total width of periodic windows is larger than for prime periods.

5. Conclusions

A systematic method to find all low-period windows for the quadratic map has been proposed. The method has been used to find very accurate approximations of the positions of periodic windows with periods $p \leq 32$. The existence of each periodic window was confirmed and very accurate rigorous bounds of its width has been found using the

interval Newton operator. It was shown that the proposed forward shooting method is very efficient for the evaluation of the interval operator. Properties of periodic windows have been discussed and relation between the total width of period- p windows and factorization of p has been studied. In future work, we plan to extend these results to periodic windows with larger periods with the goal to improve known bounds of the measure of the set of parameter values for which the behaviour of the quadratic map is regular.

Acknowledgments

This work was supported in part by the AGH University of Science and Technology, grant no. 11.11.120.343.

References

- CAPD [2015] “CAPD library,” <http://capd.ii.uj.edu.pl/>.
- Coomes, B., Koçak, H. & Palmer, K. [1996] “Shadowing in discrete dynamical systems,” *Six Lectures on Dynamical Systems*, eds. Aulbach, A. & Colonius, F. (World Scientific), pp. 163–211.
- Day, S., Kokubu, H., Luzzatto, S., Mischaikow, K., Oka, H. & Pilarczyk, P. [2008] “Quantitative hyperbolicity estimates in one-dimensional dynamics,” *Nonlinearity* **21**, 1967–1987.
- Derrida, B., Gervois, A. & Pomeau, Y. [1978] “Iteration of endomorphisms on the real axis and representation of numbers,” *Ann. Inst. Henri Poincaré* **29**, 305–356.
- Galias, Z. [2002] “Proving the existence of long periodic orbits in 1D maps using Newton method and backward shooting,” *Topology and its Applications* **124**, 25–37.
- Galias, Z. & Garda, B. [2015] “Detection of all low-period windows for the logistic map,” *Proc. IEEE Int. Symposium on Circuits and Systems, ISCAS’15* (Lisbon), pp. 1698–1701.
- Galias, Z. & Tucker, W. [2014] “On the structure of existence regions for sinks of the Hénon map,” *Chaos: An Interdisciplinary Journal of Nonlinear Science* **24**, 013120 (14 pages).
- Lyubich, M. [2002] “Almost every real quadratic map is either regular or stochastic,” *Annals of Mathematics* **156**, 1–78.
- May, R. [1976] “Simple mathematical models with very complicated dynamics,” *Nature* **261**, 459–467.
- MPFR [2015] “GNU MPFR library,” <http://www.mpfr.org>.
- Neumaier, A. [1990] *Interval methods for systems of equations* (Cambridge University Press).
- Peitgen, H., Jürgens, H. & Saupe, D. [2004] *Chaos and Fractals: New Frontiers of Science* (Springer).
- Stoer, J. & Bulirsch, R. [2002] *Introduction to Numerical Analysis* (Springer).
- Tucker, W. & Wilczak, D. [2009] “A rigorous lower bound for the stability regions of the quadratic map,” *Physica D* **238**, 1923–1936.
- Wan-Zhen, Z., Bai-Lin, H., Guang-Rui, W. & Shi-Gang, C. [1984] “Scaling property of period-n-tupling sequences in one-dimensional mappings,” *Communications in Theoretical Physics* **3**, 283.